Imaging Science in Dentistry 2024; 54: 33-41
https://doi.org/10.5624/isd.20230169

# Deep learning system for distinguishing between nasopalatine duct cysts and radicular cysts arising in the midline region of the anterior maxilla on panoramic radiographs

Yoshitaka Kise[1,*], Chiaki Kuwada[1], Mizuho Mori[1], Motoki Fukuda[2], Yoshiko Ariji[2], Eiichiro Ariji[1]

[1]*Department of Oral and Maxillofacial Radiology, Aichi Gakuin University School of Dentistry, Nagoya, Japan*
[2]*Department of Oral Radiology, School of Dentistry, Osaka Dental University, Osaka, Japan*

## ABSTRACT

**Purpose**: The aims of this study were to create a deep learning model to distinguish between nasopalatine duct cysts (NDCs), radicular cysts, and no-lesions (normal) in the midline region of the anterior maxilla on panoramic radiographs and to compare its performance with that of dental residents.

**Materials and Methods**: One hundred patients with a confirmed diagnosis of NDC (53 men, 47 women; average age, 44.6 ± 16.5 years), 100 with radicular cysts (49 men, 51 women; average age, 47.5 ± 16.4 years), and 100 with normal groups (56 men, 44 women; average age, 34.4 ± 14.6 years) were enrolled in this study. Cases were randomly assigned to the training datasets (80%) and the test dataset (20%). Then, 20% of the training data were randomly assigned as validation data. A learning model was created using a customized DetectNet built in Digits version 5.0 (NVIDIA, Santa Clara, USA). The performance of the deep learning system was assessed and compared with that of two dental residents.

**Results**: The performance of the deep learning system was superior to that of the dental residents except for the recall of radicular cysts. The areas under the curve (AUCs) for NDCs and radicular cysts in the deep learning system were significantly higher than those of the dental residents. The results for the dental residents revealed a significant difference in AUC between NDCs and normal groups.

**Conclusion**: This study showed superior performance in detecting NDCs and radicular cysts and in distinguishing between these lesions and normal groups. ***(Imaging Sci Dent 2024; 54: 33-41)***

**KEY WORDS**: Deep Learning; Machine Learning; Jaw Diseases; Radiography, Panoramic

## Introduction

Various cyst-like lesions, which present as radiolucent areas with smooth and well-defined margins on radiographs and include cysts and benign odontogenic tumors, frequently occur in the jaws,[1-4] and radiological differentiation plays an important role in the selection of treatment methods. Some lesions, such as Stafne's bone cavity, develop site-specifically, and their location occasionally helps to differentiate them from other lesions. Nasopalatine duct cysts (NDCs), also known as incisive canal cysts, are the most common non-odontogenic cyst occurring in the midline region of the anterior maxilla.[5,6] NDCs are believed to arise from epithelial remnants of the nasopalatine duct and are radiographically characterized as a circular or heart-shaped radiolucency in the midline area of the anterior maxilla. Depending on anatomical variations of the nasopalatine duct,[7,8] NDCs are occasionally located asymmetrically along the midline and close to the root apices of the incisors. Therefore, they are often indistinguishable from periapical lesions of the maxillary incisors on radiographs.[9-12] NDCs are generally treated by excision, and adjacent teeth can be preserved if they are not involved. In contrast, radicular cysts are frequently treated by excision with extraction of the causative teeth. Sometimes, they can be treated solely

Received August 4, 2023; Revised October 31, 2023; Accepted November 22, 2023
Published online December 13, 2023
*Correspondence to : Dr. Yoshitaka Kise
Department of Oral and Maxillofacial Radiology, Aichi Gakuin University School of Dentistry, 2-11 Suemori-dori, Chikusa-ku, Nagoya 464-8651, Japan
Tel) 81-52-759-2165, E-mail) kise@dpc.agu.ac.jp

by root canal therapy (non-surgical or surgical); Anyhow, the causative teeth need to be treated for healing to occur. Although some authors have advocated the use of computed tomography (CT), cone beam CT for dental use, and magnetic resonance imaging to differentiate between these lesions,[5,12-14] there is still an important role for panoramic radiography because of its low radiation exposure,[15] low cost, and convenience.

In recent years, research on diagnostic imaging using deep learning systems has been rapidly progressing, and its usefulness in the maxillofacial region has been reported using panoramic radiographs.[16-39] A deep learning system is an artificial intelligence machine learning method that allows a computer to learn tasks in the same way as humans, based on a neural network system that imitates the neurons in the human brain. Many authors have reported the clinical usefulness of deep learning systems for panoramic diagnosis, and several studies have addressed the classification of cyst-like lesions including NDCs and radicular cysts.[35,37,38] However, the performance of these deep learning systems is insufficiently verified for the midline region of the anterior maxilla. This may be partially attributable to the anatomical complexity of this region and certain features of panoramic images, including the superimposed cervical spine and the thin imaging layer. These problems need to be solved as the next step in the development of fully automatic deep learning systems for panoramic radiographs. Additionally, the lesions should be initially compared with images with normal appearance and then accurately detected and classified.

Taken together, the aims of this study were to create a deep learning model specialized in distinguishing between NDCs, radicular cysts, and no-lesions (normal) in the midline region of the anterior maxilla on panoramic radiographs and to evaluate its performance in comparison with diagnoses by dental residents.

## Materials and Methods

The study design was approved by the Ethics Committee of our university (approval number 496) and was planned according to the ethical standards of the Helsinki Declaration. This was a non-invasive, observational study using only anonymized panoramic radiographs from a database. By using opt-out consent, subjects were given the opportunity to refuse to participate in the study. The Ethics Committee of our university waived the requirement for informed consent from all participants.

### Subjects

The subjects were retrospectively selected from the image database of patients who visited our institution from February 2002 to May 2022. Patients with radiolucent cyst-like lesions in the midline region of the anterior maxilla on panoramic radiographs were included. Of these, lesions with a maximum diameter of 10 mm or more occurring in the area of the central and lateral incisors were selected. Patients with a history of previous surgery or malignant lesions were excluded. Poor quality images were also excluded. Consequently, the study included 100 NDCs (53 men, 47 women; average age, 44.6 ± 16.5 years) and 100 radicular cysts (49 men, 51 women; average age, 47.5 ± 16.4 years) (Table 1). All cases of radicular cysts and 31 cases of NDCs were surgically removed and histopathologically diagnosed. The 69 cases of NDCs that were judged not to require aggressive treatment and were simply followed up, were also included. For these cases, two radiologists with more than 10 years' experience made the diagnosis based on the CT appearance and reached a consensus after discussion if the diagnoses were inconsistent. Additionally, 100 patients (56 men, 44 women; average age, 34.4 ± 14.6 years) without lesions in the maxillary anterior region were used as a normal group. Cases were randomly assigned to the training datasets (80%) and the test dataset (20%). Then, 20% of the training data were randomly assigned as validation data.

### Imaging data

Panoramic radiographs of all the patients were obtained using a Veraview Epocs system (J Morita Mfg Corp., Kyoto,

**Table 1.** Summary of subjects and number of training, validation, and test datasets

| | Number of patients (male, female) | Age | Training dataset | Validation dataset | Test dataset |
|---|---|---|---|---|---|
| Nasopalatine duct cyst | 100 (53, 47) | 44.6 ± 16.5 | 64 | 16 | 20 |
| Radicular cyst | 100 (49, 51) | 47.5 ± 16.4 | 64 | 16 | 20 |
| Normal | 100 (56, 44) | 34.4 ± 14.6 | 64 | 16 | 20 |
| Total | 300 | 42.1 ± 15.8 | 192 | 48 | 60 |

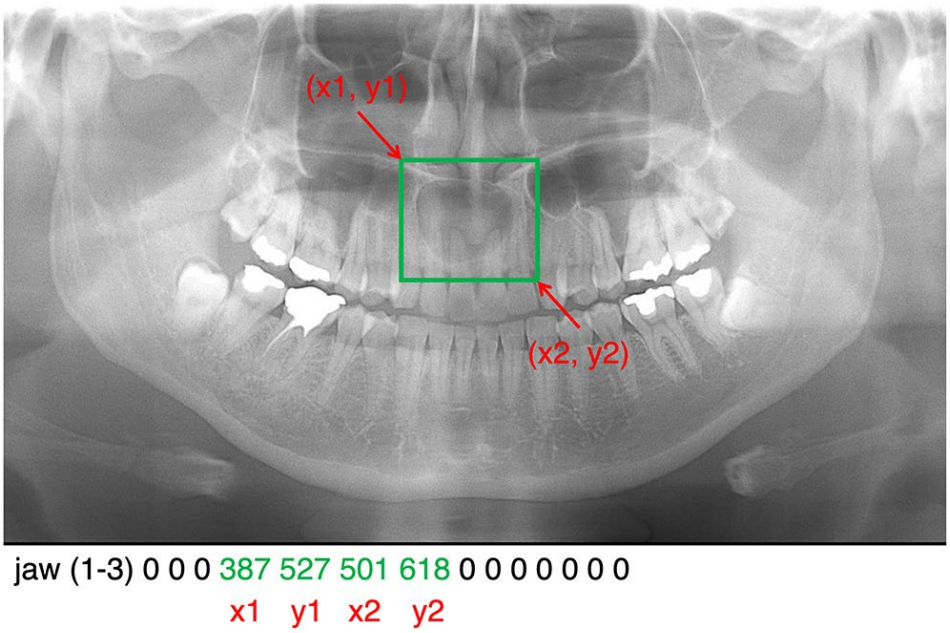


**Fig. 1.** Example of labeling procedure. A region of interest of an arbitrary size was set for the lesion, and the x and y coordinates of the upper left corner and the lower right corner were recorded. A label including the lesion class name (jaw1-3) and the x and y coordinates of the upper left and lower right corners was created in text format.

Japan). The standard parameters were tube voltage of 75 kV, tube current of 9 mA, and acquisition time of 16 seconds. The 300 selected images were downloaded in tagged image file format (TIFF) from the hospital imaging database and were then converted from TIFF format to portable network graphics format (PNG). Therefore, all images were uncompressed. Finally, all images were cropped to a size of 900 × 900 pixels to adapt to the DetectNet standard used in this verification.

### Labeling procedure

For each image, a square region of interest surrounding the lesion was manually established by an experienced radiologist using ImageJ software (National Institute of Health, Bethesda, MD, USA). The coordinates of the upper left and lower right corners of the square were recorded in text format (Fig. 1). The class names were determined as jaw1 for NDCs, jaw2 for radicular cysts, and jaw3 for normal groups.

### Deep learning system

The NVIDIA GeForce GTX GPU workstation (Nvidia Corp., Santa Clara, CA, USA) with 128 GB of memory and 11 GB of GPU was used for the deep learning process. This study used the DetectNet neural network for object detection on the DIGITS training system version 5.0 (NVIDIA; https://developer.ndivia.com/digits) and the Caffe framework. We used the adaptive moment estimation (Adam) solver, with 0.0001 as the base learning rate. The training processes were conducted for 1000 epochs, and a learning model was acquired. To investigate the inter-model agreement, the training model was created twice using the same data. The fully convolutional network (FCN) sub-network of DetectNet has the same structure as GoogLeNet without the data input layers, final pooling layer, and output layers, and we used a pretrained GoogLeNet model in this study (Fig. 2).[40,41]

### Diagnostic performance of the deep learning system

The learning model was evaluated with test data including the three classes. When a cyst-like lesion was predicted to exist, the colored bounding boxes were superimposed over the panoramic images with different colors according to the classifications. The predicted bounding boxes were displayed in red for jaw1 (NDC) and light blue for jaw2 (radicular cyst) (Fig. 3). No bounding box was displayed for the normal groups. Intersection over unions (IoUs), which is the most popular evaluation metric used in object detection, was calculated based on the predicted and ground truth areas. In this study, the IoU threshold for determining whether the lesions could be correctly detected was set at 0.6. The ground truth area was determined by an experienced radiologist in a manner similar to the establishment of the region of interest in the labeling procedure. To evaluate the performance, the recall (sensitivity), precision (positive predictive value), F1 score (harmonic mean of recall and precision), and accuracy were calculated from the confusion matrix. Furthermore, receiver operating characteristic (ROC) anal-

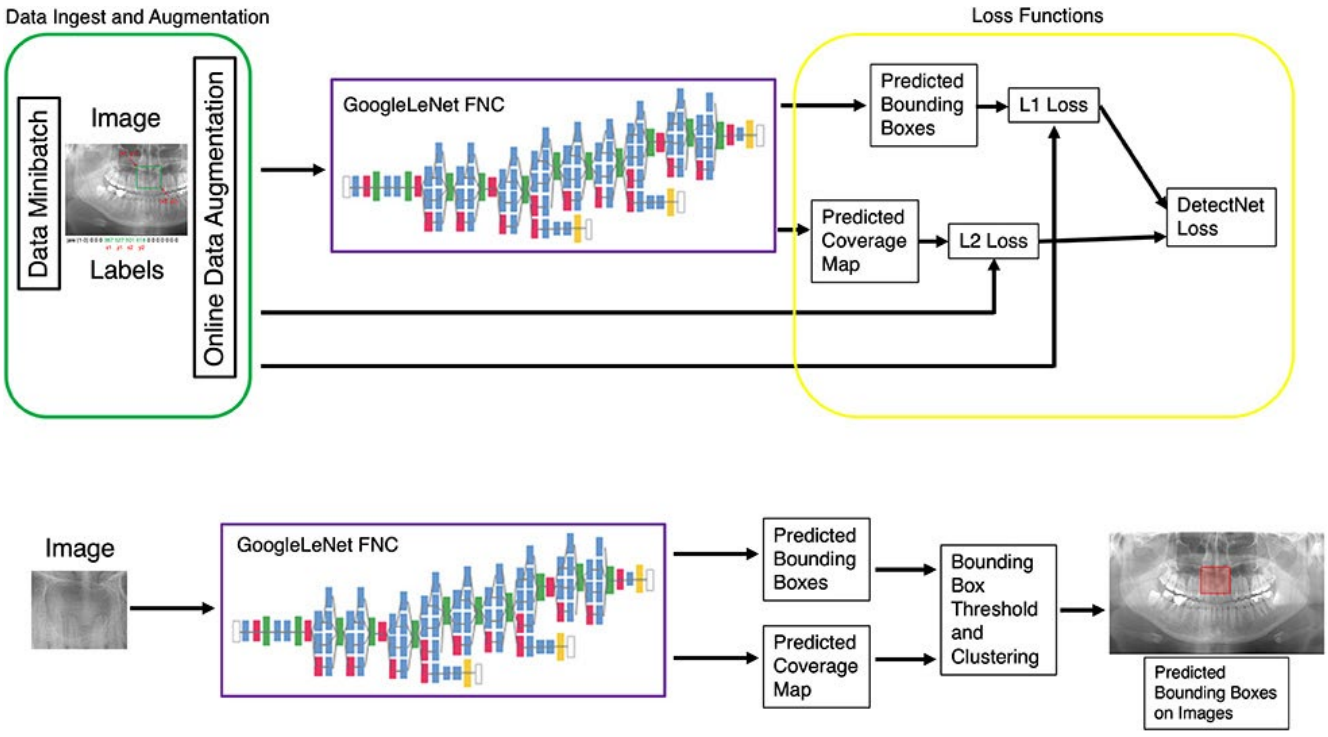


**Fig. 2.** DetectNet architecture. Data layers ingest three training images and labels and a transformer layer applies online data augmentation. A fully-convolutional network (FCN) performs feature extraction and prediction of object classes and bounding boxes per grid square. Loss functions simultaneously measure the error in the two tasks of predicting the object coverage and object bounding box corners per grid square. Testing processes are shown in the bottom row. A clustering function produces the final set of predicted bounding boxes during validation. The predicted bounding box is the area in which the learning model predicts the presence of a lesion. When the presence of a radiolucent lesion is predicted, the colored bounding boxes are superimposed over the panoramic radiographs.

ysis was performed for each lesion and the area under the curve (AUC) was calculated. ROC analysis was made with one class against the other two classes (e.g., NDC vs radicular cyst and normal group).

### Diagnostic performance of dental residents

Two dental residents with less than 10 months' experience of interpreting panoramic radiographs independently evaluated the test images (20 NDCs, 20 radicular cysts and 20 normal groups) used in the inference process of the learning model. Before making actual assessments, they were calibrated using 15 images (5 NDCs, 5 radicular cysts, and 5 normal groups) that were not used to create the learning models. Each test image was randomly evaluated using Microsoft PowerPoint on a personal computer. The confusion matrix was created from the obtained results and the recall, precision, F1 score, and accuracy were calculated. ROC analysis was also performed for each lesion and the AUC was calculated. The AUCs were compared between the deep learning system and the residents.

### Statistical analysis

Differences between the AUC values were tested using chi-square analysis with the JMP statistical software package (version 16.2.0; SAS Institute, Cary, NC, USA). The significance level was set to $p<0.05$. Inter-observer/model agreement was assessed with κ values. A κ value of $<0.20$ indicated poor agreement, 0.21 to 0.40 indicated fair agreement, 0.41 to 0.60 indicated moderate agreement, 0.61 to 0.80 indicated good agreement, and 0.81 to 1.00 indicated excellent agreement.

## Results

Summaries of the cyst detection performance of the deep learning system and residents are shown in Tables 2 and 3, respectively. Confusion matrix analyses showed that the recall, precision, and F1 scores for NDCs identified using the deep learning system were 0.83, 0.92, and 0.87, respectively; those for the radicular cyst were 0.85, 0.94, and 0.89, respectively; and those for the normal group were 0.95, 0.79, and 0.86, respectively. The accuracies of the deep learning

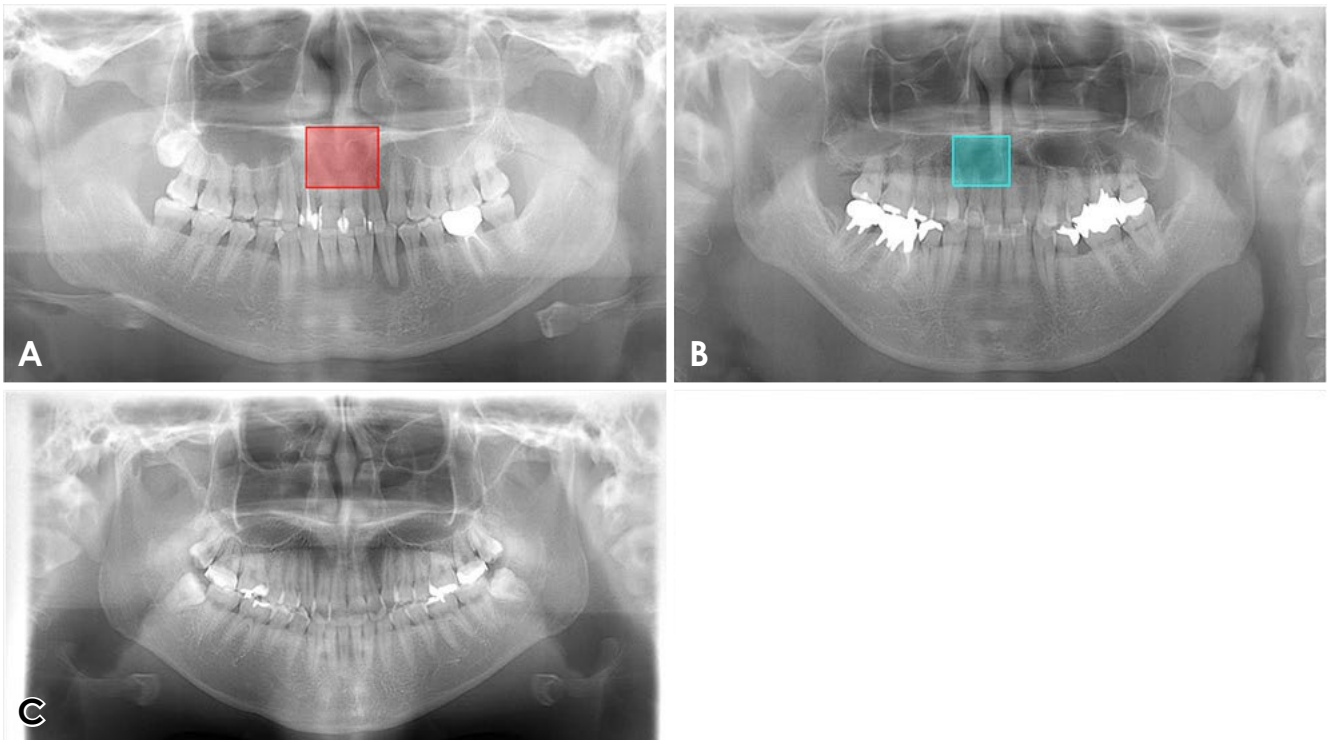


**Fig. 3.** Examples of successful detection of lesions in the maxillary anterior region. The predicted bounding boxes are displayed in red for a nasopalatine duct cyst (A), in light blue for a radicular cyst (B), and no bounding box for the normal groups (C).

**Table 2.** Confusion matrix of deep learning system

| Deep learning system | Nasopalatine duct cyst | Radicular cyst | Normal | Recall | Precision | F1 score |
|---|---|---|---|---|---|---|
| Nasopalatine duct cyst | 33 | 2 | 5 | 0.83 | 0.92 | 0.87 |
| Radicular cyst | 1 | 34 | 5 | 0.85 | 0.94 | 0.89 |
| Normal | 2 | 0 | 38 | 0.95 | 0.79 | 0.86 |
| | | | | | Accuracy | 0.88 |

**Table 3.** Confusion matrix of dental residents

| Dentists | Nasopalatine duct cyst | Radicular cyst | Normal | Recall | Precision | F1 score |
|---|---|---|---|---|---|---|
| Nasopalatine duct cyst | 27 | 10 | 3 | 0.68 | 0.79 | 0.73 |
| Radicular cyst | 3 | 36 | 1 | 0.90 | 0.71 | 0.79 |
| Normal | 4 | 5 | 31 | 0.78 | 0.89 | 0.83 |
| | | | | | Accuracy | 0.78 |

system and dental residents were 0.88 and 0.78, respectively. The performance of the deep learning system was superior to that of the residents except for the recall of radicular cysts.

The AUCs for the NDC, radicular cyst, and normal groups identified using the deep learning system were 0.894, 0.913, and 0.913, respectively. The AUCs for NDCs ($p=0.0013$) and radicular cysts ($p=0.0380$) identified using the deep learning system were significantly higher than the AUCs for those identified by the residents (Table 4 and Fig. 4). Among the residents, there was a significant difference in the AUCs between the NDC and normal groups ($p=$

**Table 4.** Comparison of diagnostic performance in area under the curves (AUCs)

| | Deep learning system | | | Residents | | |
|---|---|---|---|---|---|---|
| | Nasopalatine duct cyst | Radicular cyst | Normal | Nasopalatine duct cyst | Radicular cyst | Normal |
| AUC | 0.894[a] | 0.913[b] | 0.913 | 0.794[a,c] | 0.856[b] | 0.863[c] |

a, b, c: values with the same characters denote significant differences with $p < 0.05$

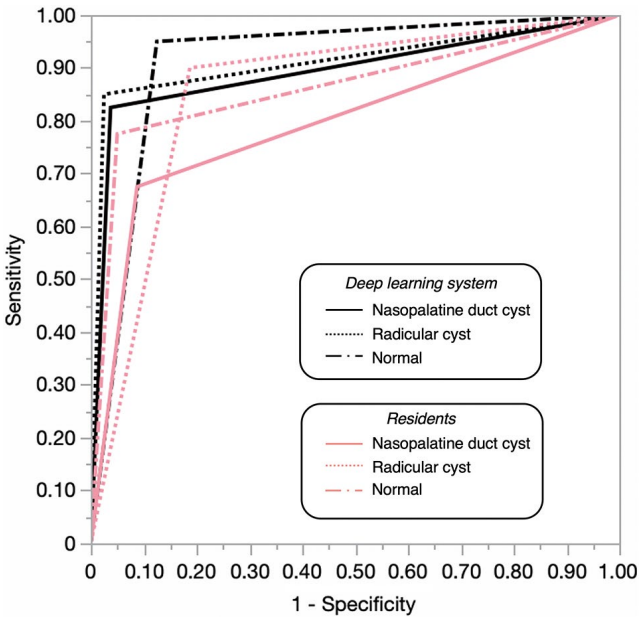


**Fig. 4.** Receiver operating characteristic curves for each lesion for the deep learning system and for the dental residents. The areas under the curve of a nasopalatine duct cyst, a radicular cyst, and the normal group by the deep learning system are 0.894, 0.913, and 0.913 respectively. Those of the dental residents are 0.794, 0.856, and 0.863, respectively.

0.0089). Inter-model and inter-observer agreements were 0.93 (excellent) and 0.57 (moderate), respectively.

## Discussion

Several deep learning studies have addressed cyst-like lesions of the maxilla on panoramic radiographs.[35,37,38] Yang et al.[35] evaluated the performance of You Only Look Once (YOLO) v2. for cyst-like lesions in the jaws including the anterior maxilla and reported superior performance. However, NDCs and radicular cysts were not included. Kwon et al.[38] also used a deep learning system for diagnosing cyst-like lesions of the jaws including the maxilla. Although their study dealt with radicular cysts, NDCs were not included, and the location of the lesions was not taken into account. The performance of deep learning object detection technology was examined for identifying maxillary cyst-like lesions on panoramic radiographs.[37] Although the test data included radicular cysts and NDCs, the classification performance was tested only between radicular cysts and other lesions because of the small number of NDCs and other lesions, resulting in a relatively high recall (0.80) of radicular cysts in the whole maxilla. However, the specific value for the anterior maxilla was not reported for radicular cysts. Furthermore, although the performance was superior for all lesions arising in the anterior maxilla compared with the performance for those in the posterior region, the specific value of this region for radicular cysts was not provided. This is the first study to show improved performance in distinguishing between NDCs and radicular cysts arising in the midline region of the anterior maxilla with an accuracy of 0.88 and AUCs of approximately 0.9 for all three groups (NDCs, radicular cysts, and normal groups).

In the dental residents group, the performances for radicular cysts and normal groups were relatively high compared with those for NDCs. This is probably because of the residents lack of experience in interpreting panoramic radiographs. Experienced radiologists usually interpret images based on morphologic internal and peripheral characteristics, and their diagnostic performance depends on their experience. The residents had little experience, and could not effectively differentiate between the appearance of NDCs and radicular cysts during their short time interpreting panoramic radiographs. In contrast, because periapical lesions are the most common cyst-like lesions in the jaw,[2] the residents had some experience in discerning radicular cysts as well as the images of normal groups. The residents misdiagnosed 25.0% (10/40) of NDCs as radicular cysts. This means that NDCs could be inappropriately treated by inexperienced dentists as reported by Aparna et al.[11] They concluded that appropriate interpretation of clinical, radiographic, and histological features offers pertinent clues to the diagnosis of NDCs. Therefore, the treatment procedures should be determined after interpretation of all perspectives, and a deep learning system may be useful as such a support.

Comparing the deep learning system error cases (NDCs, 7; radicular cysts, 6; normal, 2) with those of the residents, the agreement was approximately 50%. The contents of the deep learning system are a black box and its inner workings are unknown. Probably looking at the site and morphology, but not actually knowing. It is also probable that the deep learning system makes decisions based on different information (e.g., "different aspects of that morphology") than humans.

The performance of deep learning systems for diagnostic imaging is generally reported to be similar to that of experienced radiologists and often superior to that of inexperienced observers, such as residents, indicating that deep learning systems could help residents interpret images.[32,42-45] A previous study of deep learning systems for panoramic diagnosis of maxillary sinusitis[32] found that the AUCs were 0.875, 0.896, and 0.767 for the deep learning system, experienced radiologists, and dental residents, respectively, with a significant difference between the scores of residents and the other two groups. Similar results were reported for diagnosis of temporomandibular arthritis by panoramic radiography and three-dimensional contact status between the mandibular third molar and the mandibular canal.[44,45] Even though the performance of experienced radiologists was not evaluated in the present study, our findings support the previous conclusions, verifying the effectiveness of deep learning systems for assisting inexperienced observers.

Inter-model agreement was excellent at 0.93, while inter-observer agreement was moderate at 0.57. The deep learning system had a highly stable performance compared with that of the residents. Taking diagnostic reliability into account, the deep learning system therefore also had the potential to provide diagnostic support to inexperienced observers.

The present study had several limitations. First, we investigated only two lesions, NDCs and radicular cysts, and we acknowledge that other lesions such as odontogenic keratocysts and ameloblastomas also occur in the midline region of the anterior maxilla. Therefore, verification of our findings including these lesions is necessary before clinical applications can be considered. Second, this study investigated only radiolucent lesions. The deep learning model should also be studied in relation to radiopaque lesions. Third, this study used only DetectNet. Although DetectNet has a proven track record in object detection and has a reliable accuracy, the use of modern neural networks (e.g., YOLOv7) and comparisons of several neural networks are needed in future studies. Fourth, only two residents were enrolled in the study, and each only did one test. It was possible to determine inter-observer agreement but not intra-observer agreement. Therefore, multiple tests and more residents are needed to improve reliability and reproducibility. Fifth, we did not validate the findings using experienced radiologists. Comparison between their findings and those of the deep learning system is important, but the diagnostic accuracy of the deep learning system in this study was nonetheless very high (AUC $\approx$ 0.9). Therefore, the deep learning system could be used to support inexperienced residents. Finally, the datasets were so small that the model's generalizability could not be verified. Ensuring generalizability is a challenging yet crucial issue in artificial intelligence modeling. The primary method to ensure this involves combining data from diverse centers with different vendors across various populations. To achieve this and mitigate the limitation of small sample size, previous studies have employed data augmentation techniques. Additionally, others have attempted to address vendor-specific interference by incorporating data from multiple vendors. Therefore, future studies should include a cross-institutional validation test with collaboration from multiple facilities.

In conclusion, we investigated the performance of a deep learning system in detecting cyst-like lesions in the midline region of the anterior maxilla. This study showed superior performance in detecting NDCs and radicular cysts and in distinguishing between these cysts and normal groups. The results suggest that the deep learning system can provide support for inexperienced residents.

**Conflicts of Interest:** None

## Acknowledgments

We thank Edanz (https://jp.edanz.com/ac) for editing drafts of this manuscript.

## References

1. Robinson RA. Diagnosing the most common odontogenic cystic and osseous lesions of the jaws for the practicing pathologist. Mod Pathol 2017; 30(s1): S96-103.
2. Koivisto T, Bowles WR, Rohrer M. Frequency and distribution of radiolucent jaw lesions: a retrospective analysis of 9,723 cases. J Endod 2012; 38: 729-32.
3. Yeung AW. Radiolucent lesions of the jaws: an attempted demonstration of the use of co-word analysis to list main similar pathologies. Int J Environ Res Public Health 2022; 19: 1933.
4. Marmary Y, Kutiner G. A radiographic survey of periapical jawbone lesions. Oral Surg Oral Med Oral Pathol 1986; 61: 405-8.
5. Escoda Francolí J, Almendros Marqués N, Berini Aytés L, Gay

Escoda C. Nasopalatine duct cyst: report of 22 cases and review of the literature. Med Oral Patol Oral Cir Bucal 2008; 13: E438-43.
6. Elliott KA, Franzese CB, Pitman KT. Diagnosis and surgical management of nasopalatine duct cysts. Laryngoscope 2004; 114: 1336-40.
7. Bornstein MM, Balsiger R, Sendi P, von Arx T. Morphology of the nasopalatine canal and dental implant surgery: a radiographic analysis of 100 consecutive patients using limited cone-beam computed tomography. Clin Oral Implants Res 2011; 22: 295-301.
8. Cicciù M, Grossi GB, Borgonovo A, Santoro G, Pallotti F, Maiorana C. Rare bilateral nasopalatine duct cysts: a case report. Open Dent J 2010; 4: 8-12.
9. Faitaroni LA, Bueno MR, Carvalhosa AA, Mendonça EF, Estrela C. Differential diagnosis of apical periodontitis and nasopalatine duct cyst. J Endod 2011; 37: 403-10.
10. Suter VG, Büttner M, Altermatt HJ, Reichart PA, Bornstein MM. Expansive nasopalatine duct cysts with nasal involvement mimicking apical lesions of endodontic origin: a report of two cases. J Endod 2011; 37: 1320-6.
11. Aparna M, Chakravarthy A, Acharya SR, Radhakrishnan R. A clinical report demonstrating the significance of distinguishing a nasopalatine duct cyst from a radicular cyst. BMJ Case Rep 2014; 2014: bcr2013200329.
12. Levy DH, Dinur N, Becker T, Azizi H, Ben Itzhak J, Solomonov M. Use of cone-beam computed tomography as a critical component in the diagnosis of an infected nasopalatine duct cyst mimicking chronic apical abscess: a case report. J Endod 2021; 47: 1177-81.
13. Pevsner PH, Bast WG, Lumerman H, Pivawer G. CT analysis of a complicated nasopalatine duct cyst. N Y State Dent J 2000; 66: 18-20.
14. Spinelli HM, Isenberg JS, O'Brien M. Nasopalatine duct cysts and the role of magnetic resonance imaging. J Craniofac Surg 1994; 5: 57-60.
15. Wrzesień M, Olszewski J. Absorbed doses for patients undergoing panoramic radiography, cephalometric radiography and CBCT. Int J Occup Med Environ Health 2017; 30: 705-13.
16. Kwak GH, Kwak EJ, Song JM, Park HR, Jung YH, Cho BH, et al. Automatic mandibular canal detection using a deep convolutional neural network. Sci Rep 2020; 10: 5711.
17. Kats L, Vered M, Blumer S, Kats E. Neural network detection and segmentation of mental foramen in panoramic imaging. J Clin Pediatr Dent 2020; 44: 168-73.
18. Lee A, Kim MS, Han SS, Park P, Lee C, Yun JP. Deep learning neural networks to differentiate Stafne's bone cavity from pathological radiolucent lesions of the mandible in heterogeneous panoramic radiography. PLoS One 2021; 16: e0254997.
19. Choi E, Lee S, Jeong E, Shin S, Park H, Youm S, et al. Artificial intelligence in positioning between mandibular third molar and inferior alveolar nerve on panoramic radiography. Sci Rep 2022; 12: 2456.
20. Yang S, Lee H, Jang B, Kim KD, Kim J, Kim H, et al. Development and validation of a visually explainable deep learning model for classification of C-shaped canals of the mandibular second molars in periapical and panoramic dental radiographs. J Endod 2022; 48: 914-21.
21. Tassoker M, Öziç MÜ, Yuce F. Comparison of five convolutional neural networks for predicting osteoporosis based on mandibular cortical index on panoramic radiographs. Dentomaxillofac Radiol 2022; 51: 20220108.
22. Jeon SJ, Yun JP, Yeom HG, Shin WS, Lee JH, Jeong SH, et al. Deep-learning for predicting C-shaped canals in mandibular second molars on panoramic radiographs. Dentomaxillofac Radiol 2021; 50: 20200513.
23. Fukuda M, Inamoto K, Shibata N, Ariji Y, Yanashita Y, Kutsuna S, et al. Evaluation of an artificial intelligence system for detecting vertical root fracture on panoramic radiography. Oral Radiol 2020; 36: 337-43.
24. Ariji Y, Yanashita Y, Kutsuna S, Muramatsu C, Fukuda M, Kise Y, et al. Automatic detection and classification of radiolucent lesions in the mandible on panoramic radiographs using a deep learning object detection technique. Oral Surg Oral Med Oral Pathol Oral Radiol 2019; 128: 424-30.
25. Kise Y, Ariji Y, Kuwada C, Fukuda M, Ariji E. Effect of deep transfer learning with a different kind of lesion on classification performance of pre-trained model: verification with radiolucent lesions on panoramic radiographs. Imaging Sci Dent 2023; 53: 27-34.
26. Nishiyama M, Ishibashi K, Ariji Y, Fukuda M, Nishiyama W, Umemura M, et al. Performance of deep learning models constructed using panoramic radiographs from two hospitals to diagnose fractures of the mandibular condyle. Dentomaxillofac Radiol 2021; 50: 20201611.
27. Hiraiwa T, Ariji Y, Fukuda M, Kise Y, Nakata K, Katsumata A, et al. A deep-learning artificial intelligence system for assessment of root morphology of the mandibular first molar on panoramic radiography. Dentomaxillofac Radiol 2019; 48: 20180218.
28. Ariji Y, Mori M, Fukuda M, Katsumata A, Ariji E. Automatic visualization of the mandibular canal in relation to an impacted mandibular third molar on panoramic radiographs using deep learning segmentation and transfer learning techniques. Oral Surg Oral Med Oral Pathol Oral Radiol 2022; 134: 749-57.
29. Kotaki S, Nishiguchi T, Araragi M, Akiyama H, Fukuda M, Ariji E, et al. Transfer learning in diagnosis of maxillary sinusitis using panoramic radiography and conventional radiography. Oral Radiol 2023; 39: 467-74.
30. Mori M, Ariji Y, Katsumata A, Kawai T, Araki K, Kobayashi K, et al. A deep transfer learning approach for the detection and diagnosis of maxillary sinusitis on panoramic radiographs. Odontology 2021; 109: 941-8.
31. Kuwana R, Ariji Y, Fukuda M, Kise Y, Nozawa M, Kuwada C, et al. Performance of deep learning object detection technology in the detection and diagnosis of maxillary sinus lesions on panoramic radiographs. Dentomaxillofac Radiol 2021; 50: 20200171.
32. Murata M, Ariji Y, Ohashi Y, Kawai T, Fukuda M, Funakoshi T, et al. Deep-learning classification using convolutional neural network for evaluation of maxillary sinusitis on panoramic radiography. Oral Radiol 2019; 35: 301-7.
33. Kuwada C, Ariji Y, Kise Y, Funakoshi T, Fukuda M, Kuwada T, et al. Detection and classification of unilateral cleft alveolus with and without cleft palate on panoramic radiographs using a deep learning system. Sci Rep 2021; 11: 16044.

34. Kuwada C, Ariji Y, Kise Y, Fukuda M, Nishiyama M, Funakoshi T, et al. Deep-learning systems for diagnosing cleft palate on panoramic radiographs in patients with cleft alveolus. Oral Radiol 2023; 39: 349-54.
35. Yang H, Jo E, Kim HJ, Cha IH, Jung YS, Nam W, et al. Deep learning for automated detection of cyst and tumors of the jaw in panoramic radiographs. J Clin Med 2020; 9: 1839.
36. Kuwada C, Ariji Y, Fukuda M, Kise Y, Fujita H, Katsumata A, et al. Deep learning systems for detecting and classifying the presence of impacted supernumerary teeth in the maxillary incisor region on panoramic radiographs. Oral Surg Oral Med Oral Pathol Oral Radiol 2020; 130: 464-9.
37. Watanabe H, Ariji Y, Fukuda M, Kuwada C, Kise Y, Nozawa M, et al. Deep learning object detection of maxillary cyst-like lesions on panoramic radiographs: preliminary study. Oral Radiol 2021; 37: 487-93.
38. Kwon O, Yong TH, Kang SR, Kim JE, Huh KH, Heo MS, et al. Automatic diagnosis for cysts and tumors of both jaws on panoramic radiographs using a deep convolution neural network. Dentomaxillofac Radiol 2020; 49: 20200185.
39. Song IS, Shin HK, Kang JH, Kim JE, Huh KH, Yi WJ, et al. Deep learning-based apical lesion segmentation from panoramic radiographs. Imaging Sci Dent 2022; 52: 351-7.
40. Tao A, Barker J, Sarathy S. DetectNet: deep neural network for object detection in DIGITS. 2016 Aug 11 [cited 2023 Aug 3]. In: NVIDIA Developer. Technical Blog [Internet]. Santa Clara: NVIDIA Corp. Available from: https://developer.nvidia.com/blog/detectnet-deep-neural-network-object-detection-digits/.
41. Barker J, Prasanna S. Deep learning for object detection with DIGITS. 2016 Aug 11 [cited 2023 Aug 3]. In: NVIDIA Developer. Technical Blog [Internet]. Santa Clara: NVIDIA Corp. Available from: https://developer.nvidia.com/blog/deep-learning-object-detection-digits/.
42. Kise Y, Ikeda H, Fujii T, Fukuda M, Ariji Y, Fujita H, et al. Preliminary study on the application of deep learning system to diagnosis of Sjögren's syndrome on CT images. Dentomaxillofac Radiol 2019; 48: 20190019.
43. Kise Y, Shimizu M, Ikeda H, Fujii T, Kuwada C, Nishiyama M, et al. Usefulness of a deep learning system for diagnosing Sjögren's syndrome using ultrasonography images. Dentomaxillofac Radiol 2020; 49: 20190348.
44. Nozawa M, Ariji Y, Fukuda M, Kise Y, Naitoh M, Nishiyama M, et al. Use of a deep learning system for diagnosis of degenerative disease of the temporomandibular joint on panoramic radiographs. J Jpn Soc Temporomandibular Joint 2020; 32: 55-64.
45. Fukuda M, Kise Y, Naitoh M, Ariji Y, Fujita H, Katsumata A, et al. Deep learning system to predict the three-dimensional contact status between the mandibular third molar and mandibular canal using panoramic radiographs. Oral Sci Int (in press).